RIETI Discussion Paper Series 22-E-011

Exploring the Dynamic Relationship between Mobility and the Spread of COVID-19, and the Role of Vaccines

INOUE, Tomoo
Seikei University

OKIMOTO, Tatsuyoshi
RIETI

Research Institute of Economy, Trade & Industry, IAA

The Research Institute of Economy, Trade and Industry
https://www.rieti.go.jp/en/

RIETI Discussion Paper Series 22-E-011
February 2022

Exploring the dynamic relationship between mobility and the spread of COVID-19, and the role of vaccines*

Tomoo Inoue†
Faculty of Economics, Seikei University

and

Tatsuyoshi Okimoto‡
Crawford School of Public Policy, Australian National University
Research Institute of Economy, Trade and Industry (RIETI)

Abstract
The novel coronavirus disease 2019 (COVID-19) outbreak has caused great turmoil around the world and is yet to be contained. Mitigating the number of people infected by COVID-19 remains a major policy goal for several countries. The purpose of this study is to analyze the dynamic relationship between mobility and the rate of change in the number of new infections in Japan. Another goal is to evaluate the effects of various policies, such as human mobility control and vaccination, as well as the impact of climate factors on the number of infections. The analysis reveals a strong positive relationship between the growth rate of the number of infections and mobility. Our results also indicate that the declaration of the state emergency effectively controlled the infection, although the effect seems to be weaker with additional declarations of a state of emergency. On the effect of vaccination, the results find little effect of vaccination on reducing the spread of infection through a reduction in susceptible population, but it has significantly weakened the mobility-spread relationship, suggesting that it may be useful in implementing economic revitalization policies.

Keywords: COVID-19, vaccination, impulse response analysis, SIR model, mobility control policy
JEL classification: C23, H12, I18

---

* This paper is part of the results of a research project by the second author at the Research Institute of Economy, Trade and Industry (RIETI). We would like to thank Shiba Suzuki and Vu Tuan Khai for many useful comments on the original draft of this paper. This research was partially supported by a grant-in-aid from Zengin Foundation for Studies on Economics and Finance (2021).
† Professor, Faculty of Economics, Seikei University, 3-3-1, Kichijoji Kitamachi, Musashino, Tokyo 180-8633, Japan. E-mail: inoue@econ.seikei.ac.jp
‡ Associate Professor, Crawford School of Public Policy, Australian National University, and Visiting Fellow, RIETI, 132 Lennox Crossing, ANU, Acton, ACT 2601, Australia. E-mail: tatsuyoshi.okimoto@anu.edu.au.

1 Introduction

The coronavirus disease 2019 (COVID-19) outbreak at the end of 2019 has caused great turmoil worldwide and is yet to be contained. Therefore, mitigating the number of people infected by the virus remains a major policy goal for several countries. Restricting the flow of people is one of the most effective policies to control infection; as a result, various policies have been implemented in several countries. The most stringent policies include entry restrictions and city blockades, which were initially implemented in, among other countries, the United States and the United Kingdom. In Japan, where city blockades are impossible, the main policies include declaring a state of emergency (SOE) and restricting the business capacity of restaurants.[*1] At the same time, remote work has been promoted worldwide, and policies encouraging people to stay at home have been implemented. Furthermore, while such measures are being implemented, vaccines have been developed, and the promulgation of vaccination has become important not only to control infections but also to resume economic activities. In fact, as vaccination progresses, some countries are easing their policies to control human mobility and promoting policies to revitalize economic activities. As described above, several policies have been implemented in response to COVID-19, but the effects of these policies remain unverified: Sufficient research has not yet been conducted. In addition, most studies assessing the policy effects are simulation-based, and it is essential to conduct studies that verify the effects of policies based on actual observable data. Given these circumstances, the purpose of this study is to clarify the dynamic relationship between human mobility and the rate of change in the number of new infections in Japan and to understand the effects of various forms of mobility

[*1] The declaration of a state of emergency issued by the Japanese government is not legally binding and carries no penalties such as fines or arrests. However, since many people complied with the Japanese government's verbal "request" to refrain from going out, Watanabe and Yabu (2021) read it as a "voluntary lockdown."

control policies and vaccines on the spread of COVID-19 through empirical analysis based on actual observable data.

Research is beginning to show COVID-19's impact on economic activities and the effects of various mobility control policies enacted to reduce the spread. In particular, studies on COVID-19's impact on the economy and mobility include those by Brodeur et al. (2021), Davis et al. (2021), Eichenbaum et al. (2021), Fujii and Nakata (2021), Fukao and Shioji (2021), Gamtkitsulashvili and Plekhanov (2021), Hoshi et al. (2021), Hosono (2021), Kubota (2021), Milani (2021), and Rungcharoenkitkul (2021). For example, Eichenbaum et al. (2021) combined the Susceptible–Infected–Recovered (SIR) model, a mathematical model of infectious diseases, with a macroeconomic model to analyze the relationship between economic choices and infectious diseases.[*2] They showed that people cut back on consumption and work to reduce the chances of being infected, which reduce the severity of the epidemic but exacerbate the size of the associated recession. Gamtkitsulashvili and Plekhanov (2021) conducted an empirical analysis of the relationship between mobility and economic activities in 53 countries and economies and found that during the pandemic, a 10% decrease in mobility tended to reduce the gross domestic product by an average of 2%. Milani (2021) used a global vector autoregression model to analyze the relationship between the number of infected people, mobility, and unemployment rates, and showed that cross-border mobility spread the infection internationally, and that the spread of the infection may have caused a decline in mobility, which in turn may have worsened the unemployment rate.

In Japan, Hoshi et al. (2021) used the Susceptible–Infectious–Recovered–Deceased

[*2] The SIR model divides a population into three stages of infection: susceptible, infected, and recovered, and models the temporal changes in infectious status in a bottom-up manner. For the application of the SIR model to economic analysis, please refer to Avery et al. (2020). The estimation and identification of models related to the SIR model are discussed in Arias et al. (2021) and Korolev (2021).

(SIRD) model, which is an extension of the SIR model that includes the mortality period, and a macroeconomic model to indicate a possibility that the policy of reducing mobility suppressed infection but increased unemployment. Similarly, based on the SIRD and macroeconomic models, Hosono (2021) showed that the flow control policy may have reduced consumption, even though it reduced infection. Using a reduced-form simple SIR macro model with time-varying parameters, Fujii and Nakata (2021) explored policy questions such as how to control infection while minimizing the economic loss in Japan. Although the model is subject to Lucas's critique, the flexible nature of their model allowed to make various policy proposals. On the other hand, based on micro-foundation, Kubota (2021) has developed a structural SIR model, and examined the consequences of policy options related to the second soft lockdown. For a more detailed explanation of the impact of COVID-19 on the economy, see Brodeur et al. (2021) and Rungcharoenkitkul (2021).

Several studies have examined the effects of mobility control policies such as social distancing, staying at home, and lockdown including Allcott et al. (2020), Fang et al. (2020), Fernàndez-Villaverde and Jones (2020), Qiu et al. (2020), Bisin and Moro (2021), Caselli et al. (2021), David and Pienknagura (2021), Jung et al. (2021), and Mendolia et al. (2021), among others. For example, Allcott et al. (2020) suggested that although the mobility control policy suppressed the flow of people, the degree of suppression was small compared to voluntary suppression, and the degree to which the flow of people explained regional differences in the number of infected people was small. In contrast, Mendolia et al. (2021) reported that although the spread of infection tended to suppress mobility voluntarily, the effect of mobility suppression policies was larger. Based on the spatial SIR model, Bisin and Moro (2021) confirmed that geographical factors contribute significantly to the spread of infection and suggested that considering geographic factors when implementing mobility control policies is important. Caselli et al. (2021) analyzed the effect of policies that curb human mobility by age and gender, and documented that the policy effect was greater for women and younger age groups. Jung et al. (2021) reported that the mobility control policy was more effective in reducing the spread of infection in areas with lower poverty rates.

Another strand of literature examined the relationship between mobility and the number of infected people include Badr et al. (2020), Harris (2020), Xiong et al. (2020), Fraser and Aldrich (2021), Glaeser et al. (2021), Shao et al. (2021), and Wilson (2021). For example, Harris (2020) estimated an SIR model using age specific mobility data in Florida, suggesting that mobility among young people may be a major contributor to the spread of infection. Glaeser et al. (2021) analyzed five cities in the United States and found that a 10% decrease in mobility tended to decrease the infection rate by 19%. Based on the SIR model, Wilson (2021) examined the dynamic relationship between mobility and the rate of change of newly infected people using local projections by Jordà (2005)[*3]. The results showed that a 1% increase in mobility at various locations may increase the number of newly infected people by 0.5% to 2%, and that an increase in the cumulative number of infected people may significantly suppress the number of newly infected people through the herd immunity effect.

Although largely related to these studies, the main contribution of the present study is to analyze the dynamic relationship between human mobility and the rate of change in the number of new infections in 20 prefectures with relatively high numbers of infections in Japan during the period from the week of July 5th, 2020, through the week of November 14th, 2021. In addition, we also examine the effects of mobility control policies, vaccination, and climatic factors on the spread of infections. In

[*3] The local projection approach semiparametrically estimates the impulse responses without specifying and estimating the underlying multivariate dynamic system. Among many applications, Chong et al. (2012) was the first application that incorporated the local projection methods to panel cointegrated system, and investiagated the Harrod-Balassa-Samuleson hypothesis of real exchange rates, based on quarterly data during the 1973Q2 through 2008Q4 for 21 OECD countries.

particular, one important deviation from the previous studies is that we examine the effects of vaccination from two different perspectives. Specifically, vaccination rates can affect the infection rates not only by reducing the susceptible population, but also by weakening the relationship between the increase in the flow of people and the rate of change in the number of newly infected people. We empirically compare both channels and provide policy implications on economic revitalization policies. Moreover, we also investigate the impacts of mobility control policies with taking a possible structural change in the effectiveness. Furthermore, we compare their effects with the voluntary restraint to see differences in the effects and their time variation. These features differentiate our study from the previous studies, making it a valuable contribution to existing literature.

The main findings of this study are summarized as follows: First, our results indicate a strong positive relationship between the growth rate of the number of infections and mobility in the major category of locations, including parks, transit stations and workplaces. In contrast, our results also show a significant negative relationship between infection growth rate and mobility in residence, suggesting the effectiveness of policies promoting staying at home. Second, our analysis reveals the remarkable change in the effects of the SOE declaration. Specifically, in the early stages of the SOE declaration, it has had a clear negative impact on the rate of change in the number of newly infected people, but in the later stages when the SOE declaration was repeatedly invoked, it has had much weaker effects on the infections. Moreover, the recent increase in the infection rate has had a suppressing effect on the subsequent spread of infection due to the voluntary restraint, and this phenomenon appears to be even stronger in the recent period, which is a great contrast to the SOE effects. Finally, our results demonstrate that vaccination rates have had no significant reducing effect on the spread of infection through a reduction in the susceptible population but have significantly weakened the relationship between the flow of people and the rate of change in the number of newly infected people, suggesting that vaccination can play an important role in implementing economic revitalization policies.

The remainder of this paper is organized as follows. Section 2 introduces the SIR model and our local projection procedure based on the SIR model. Section 3 describes the details of the data used for the analysis. Section 4 summarizes the empirical results of the benchmark model, while Section 5 reports the results of the extended model with taking an additional impact of vaccination into account. Finally, Section 6 concludes the paper.

2 Model

The SIR model is a differential equation model that captures the dynamics of infectious diseases. The SIR model divides the population into three groups according to the stage of infection—susceptible, infected, and recovered—and models the change in the state of infection over time.

This study follows Wilson (2021) and considers a discrete SIR model for the evolution of the number of infected people, as shown in the following equation:

$$\Delta I_{t+1} = (\beta_t s_t - \gamma) I_t. \tag{1}$$

where I_t is the infected population, β_t is the infection rate per unit time, s_t is the ratio of the susceptible population at time t, defined by $s_t \equiv S_t/N$, where S_t is the susceptible population, N is the total population, and γ is the removal rate by recovery or isolation per unit time.[*4] [*5]

[*4] The infection rate per unit of time is assumed to fluctuate over time due to changes in mobility, climate, and the emergence of new variants.

[*5] Eq.(1) can be regarded as a variant of the controlled Galton-Watson process, which is a state-dependent random walk process and was developed to analyze population growth processes. Important theoretical studies include Küster (1985), Keller et al. (1987), and Klebaner (1989)), among others. For its application to the macroeconomic time series, see Granger et al. (1997).

In Wilson (2021), the time interval was set to 10 days, and the aggregate values for 10 days were analyzed. In Japan, a significant weekly effect (for example, cyclicality in which the number of new positive cases decreases on the Monday of the week) has been observed in the number of new positive cases reported daily; hence, a 7-day week from Sunday to Saturday is the unit of analysis.[*6] Thus, Eq.(1) attempts to explain the increase in the number of new infections from week t to week $t+1$ based on the number of new infections, infection rate, removal rate, and susceptible population in week t. In this study, we assume $\gamma = 1$ for the removal rate, as in Wilson (2021).[*7]

Under this assumption, Eq.(1) is rewritten as:

$$I_{t+1} = I_t \beta_t s_t. \tag{2}$$

By iteratively substituting Eq.(2) forward, we can express the number of new infections h periods ahead in terms of the number of new infections at time t, the infection rate β, and the susceptible population ratio s as follows:

$$I_{t+h} = I_t(\beta_t s_t)(\beta_{t+1} s_{t+1}) \cdots (\beta_{t+h-1} s_{t+h-1}).$$

If we transform both sides of this into natural logarithms, we get:

$$\log I_{t+h} - \log I_t = \sum_{\tau=0}^{h-1} \log \beta_{t+\tau} s_{t+\tau}$$

which is further modified as:

$$\log I_{t+h} - \log I_t = \log \prod_{\tau=0}^{h-1} \beta_{t+\tau} + \sum_{\tau=0}^{h-1} \log s_{t+\tau}. \tag{3}$$

[*6] The SIR model is a mathematical model that captures the dynamic behavior of the number of infected people. However, the available data for empirical analysis are not the number of infected people, but the number of test-positive people. In this study, unless otherwise specified, the two are treated synonymously. In the empirical analysis, the number of positive cases is used instead of the number of infected cases.

[*7] This assumption implies that the infection will be discovered and recovered or isolated within 7 days of infection. Wilson (2021) set the removal rate at 10 days considering the Centers for Disease Control and Prevention study, which reported that, in most cases, the duration of infection is 10 days or less (sometimes 6 days or less), the incubation period is of several days, and there is a time interval between the actual infection and the positive test result. However, footnote 11 of Wilson (2021) also reported that a model assuming a 7-day infectious period yielded very similar results.

Here, the left-hand side represents the rate of change in the number of new infections from time t to $t+h$. On the right-hand side, the infection rate factor is represented by the first term, and the susceptible population factor is represented by the second term. In this study, we use the local projection method to analyze the impact of changes in variables at t on the rate of change in h periods ahead. However, the values of the infection rates β and susceptible population ratio s after t cannot be observed at time t. Therefore, the following assumptions are made for each of them.

First, the infection rate factors from t to h are summarized as $\beta_t^h \equiv \log \prod_{\tau=0}^{h-1} \beta_{t+\tau}$, and β_t^h is expressed as a function consisting of multiple factors identified in previous studies. Specifically, m_t, a variable representing human mobility, w_t, a weather-related variable, and the implementation of governmental policies as wel as voluntary restraint that may have a direct impact on the infection rate are considered.[*8] For the mobility data, we use the index from the Google COVID-19 Community Mobility Reports. This is explained in detail in Section 3. As for the weather factors that affect infection, we use maximum temperature and precipitation as used by Wilson (2021). However, while Wilson (2021) used temperature information to capture the point at which infectious diseases such as influenza become prevalent in winter, this study uses it from a different perspective. Specifically, we examine the relationship between the number of hot summer days and ice days and infection,[*9] considering the possibility that extreme heat or cold may lower immunity and make ventilation difficult due to room temperature control problems.[*10]

[*8] See footnote 2 of Wilson (2021) for a review of some of the studies that have analyzed the relationship between weather and the COVID-19 infection.

[*9] According to the classification by the Japan Meteorological Agency (JMA), a hot summer day is defined as a day on which the temperature goes above 30 degrees Celsius, while an ice day is defined as a day on which the temperature stays below 0 degrees Celsius. As in Wilson (2021), we also estimated a model in which the number of hot summer and ice days was replaced by the maximum weekly temperature, but the coefficient of temperature was not significant, and the impulse response analysis in Sections 4 and 5 did not show any significant difference.

[*10] Professor Koji Wada, a member of the Ministry of Health, Labour and Welfare's expert panel, said: "In addition to the increase in the number of vaccinated people, seasonal factors such as

Moreover, various governmental policies have tried to influence the infection rate, such as social distancing, wearing masks and "avoiding three densities." In this study, we will focus on the effects of "implementing a declaration of an SOE." On the other hand, rational individuals will take the necessary preventive effects based on the available information, even if the government does not restrict their actions. Therefore, if the infection situation is serious, it is expected that individuals will act with self-restraint based on their rational judgment, regardless of whether the government restricts them or not, and as a result, the spread of the infection will be reduced. Following Watanabe and Yabu (2021), we call the former the "intervention effect," and the latter the "information effect" or the "fear effect," and investigate the second effect of by referring to the most recent infection status in one's own prefecture and nationwide as information that induces self-restraint.[*11] We also examine whether the deterrent effect of SOEs and the current infection status has diminished as the situation has become more protracted.

Next, how should susceptible population factors be addressed? As a starting point for modeling, we assume that no vaccine exists and that once an individual is infected (tests positive), he or she cannot be reinfected. We also assume that there is no interregional population movement and the total population of the region is fixed at N. Then, the ratio of the susceptible population at $t+\tau$ can be defined as one minus

cooler weather have reduced the amount of activity in air-conditioned rooms, making it easier to maintain distance between people, which possibly helped." "However, we believe that it is difficult to quantify the extent to which each of the multiple factors contributed to the reduction of infection, and when the temperature drops significantly in the coming winter, the infection may spread again" (URL is: https://www3.nhk.or.jp/news/html/20211006/k10013294851000.html, 2021/10/6, Accessed: 2021/12/15).

*11 Using the "Mobile Spatial Statistics" provided by DoCoMo Insight Marketing, Watanabe and Yabu (2021) have constructed the prefecture-level daily panel data about location, by age-group and gender, and investigated the effects of the government intervention and the information on people's behavior. The observation period covered was from January 6th, 2020, through November 15th, 2020.

the ratio of the cumulative infected population to the total population, $c_{t+\tau}$:

$$s_{t+\tau} \equiv 1 - c_{t+\tau} = 1 - \frac{\sum_{j=0}^{t+\tau} I_j}{N}.$$

Next, we consider the impact of vaccination promotion on the susceptible population ratio. If we denote the number of new vaccinees (the number of people who have completed two doses of vaccination) at t by V_t, the cumulative number of vaccinees up to $t+\tau$ will be $\sum_{j=0}^{t+\tau} V_j$.[*12] However, depending on the type of vaccine, there are differences in the time required for sufficient immunity to be confirmed and in the efficacy rates of the vaccine in preventing the onset of disease.[*13] In this study, we assume that [1] the vaccine efficacy rate σ is 0.895,[*14] [2] vaccination targets uninfected individuals, [3] a proportion of vaccinated individuals σ will never be infected, and [4] once antibodies are obtained, the effect lasts at least for the duration of the analysis, but a uniform lag of two weeks is assumed until the preventive effect occurs. Under these assumptions, the susceptible population ratio at $t+\tau$, $s_{t+\tau}$, can be expressed as

$$s_{t+\tau} \equiv (1 - c_{t+\tau})(1 - \sigma\nu_{t+\tau}) = \left(1 - \frac{\sum_{j=0}^{t+\tau} I_j}{N}\right)\left(1 - \sigma\frac{\sum_{j=0}^{t+\tau-2} V_j}{N}\right)$$

where $\nu_{t+\tau}$ represents the ratio of the cumulative number of vaccinees to the total population. Finally, the right-hand side of Eq.(3), $\sum_{\tau=0}^{h-1} \log s_{t+\tau}$, is rewritten by

[*12] Note that because the vaccination of health care workers was not considered, the following analysis may underestimate the effectiveness of the vaccine in areas with large numbers of health care workers.

[*13] The efficacy of the COVID-19 vaccine in preventing the onset of disease and the time when sufficient immunity is achieved is approximately 95% and approximately 7 days after the second vaccination for Pfizer, approximately 94% and 14 days after the second vaccination for Takeda/Moderna, and about 70% and 15 days after the second vaccination for AstraZeneca. (Ministry of Health, Labour and Welfare, https://www.mhlw.go.jp/stf/seisakunitsuite/bunya/vaccine_yuukousei_anzensei.html, Accessed: 2021/12/17).

[*14] Following Fujii and Nakata (2021), we have used the efficacy rate of Pfizer vaccines after second dose, that is reported in the UK's SPI-M-O Summary on March 31st, 2021. To assess robustness, we also estimated the models assuming 0.95 efficacy rate, that was used in Wilson (2021), and obtained qualitatively similar outcomes.

assuming $c_t = c_{t+\tau}, \nu_t = \nu_{t+\tau}$ for $\tau > 0$, which implies that both the previously infected share and the vaccinated share is roughly constant over the forecast horizon, as in Wilson (2021):

$$\sum_{\tau=0}^{h-1} \log s_{t+\tau} = \underbrace{h \log(1 - c_t)}_{\tilde{c}_t^h} + \underbrace{h \log(1 - \sigma \nu_t)}_{\tilde{\nu}_t^h} \tag{4}$$

In reality, [1] vaccinations have been given to people that have been already infected prior to the administration, [2] vaccine efficacy rates may change with the emergence of new variants, and [3] antibodies may decrease, and resistance may decline as time passes from the completion of the second vaccination. However, Eq.(4) seems to be a sufficiently good approximation for the susceptible population.

The model that integrates the above is written as:

$$\begin{aligned} \log I_{i,t+h} - \log I_{it} = \sum_{\tau=0}^{P} \psi^{h\tau} m_{i,t-\tau} + \sum_{\tau=0}^{P} \delta^{h\tau} w_{i,t-\tau} + \phi^h SOE_{it} \\ + \rho^h \Delta \log I_{it} + \rho^{*h} \Delta \log I_{it}^* + \theta^h \tilde{c}_{i,t}^h + \lambda^h \tilde{\nu}_{i,t}^h + \alpha_t^h + \alpha_i^h + \epsilon_{i,t,t+h} \end{aligned} \tag{5}$$

where ψ, δ, ϕ, ρ, θ, λ, and α are the regression coefficients. $I_{i,t}$ is the number of new infections observed in prefecture i during week t (total per week), and $I_{i,t}^*$ is the the number of new infections observed outside prefecture i during week t. The infection rate factors that are explicitly included in the model are: a variable representing human mobility, m_{it}; a variable representing weather factor, w_{it}; a dummy variable representing the SOE period, SOE_{it}; and two variables representing current infection status, $\Delta \log I_{it}$ and $\Delta \log I_{it}^*$. On the other hand, the susceptible population factors are: a variable representing the effect of herd immunity due to the increase in the cumulative number of infected people, $\tilde{c}_{it}^h$; and a variable representing the effect of vaccination, $\tilde{\nu}_{it}^h$. The coefficient α_t is a time fixed effect representing such factors as the nationwide changes in infection rates due to the emergence of new variants and their spread, and the impact of nationally universal (or at least common to the sample 20 prefectures) policies other than SOEs that are not explicitly considered in Eq.(5). The coefficient α_i is a prefecture fixed effect representing the specificity and heterogeneity of each prefecture, including the following: demographics, population density, lifestyle (transportation to and from work, presence of downtown areas, etc.), health care system, external mobility, and average household size. Lastly, ϵ is an error term.

Note that the left-hand side is the rate of change in the number of new infections from t to h periods ahead. In local projection, even if the explanatory variables on the right-hand side are the same, the values of the regression coefficients differ according to the forecast horizon h on the left-hand side; hence, h is added as a superscript of the coefficients to distinguish them.

In order to capture a possible change in the people's behavior toward compulsory and voluntary suppressions, the coefficients of SOE, $\Delta \log I$, and $\Delta \log I^*$ are assumed to be different between the period up to March 2021 and the period after April 2021. Though it is somehow arbitrary, we have chosen the point of separation, since the SOE covering the Tokyo metropolitan area was lifted on March 21, 2021, as well as it is in the middle of the sample period. See Fig.5.

Eq.(5) has various devices for causal inference. One can easily imagine that there is a contemporaneous interdependence between the infection status and voluntary human mobility. For instance, an increase in mobility may cause the spread of infection, but the spread of infection may cause a decrease in human mobility. By specifying the changes of future infection rate by the present and the past variables, Eq.(5) mitigates the problem of simultaneity. Put differently, we can consider that we examine the Granger causality from the various factor to the infection rate from Eq.(5). In addition, the presence of a third factor makes it difficult to identify the causal relationship. To deal with this problem, control variables are added, if they are observable. Even if they are not directly observable, thus we face the problem of the omitted variable bias, inclusion of both prefecture-specific dummies and weekly time dummies will mitigate this risk.

Since the variables related to the susceptible population ratio are nonlinearly transformed from the original ratio using the natural logarithm, the effect of a 1% increase in the ratio on the spread of infection is different as the ratio increases. We briefly review this point here. It should be noted that the variable $\tilde{c}_{it}^h$, which represents the effect of the cumulative number of infected people, is defined as follows, as in Wilson (2021).

$$\tilde{c}_{it}^h = h \log \left(1 - \frac{\sum_{j=0}^{t} I_{ij}}{N} \right) = h \log(1 - c_{it}).$$

Therefore, in Eq.(5), the effect of increasing the infection rate by 1 unit (1%. point) is:

$$\frac{\partial(\log I_{i,t+h} - \log I_{it})}{\partial c_{it}} = \theta^h \frac{-h}{1 - c_{it}}.$$

If the infection spreads, the cumulative infected population ratio c increases, and conversely, the susceptible population ratio $(1 - c)$ decreases. Since $0 < c < 1$ during the period when uninfected people exist after the appearance of COVID-19, the increase in c reduces the value of the denominator on the right-hand side. If $\theta^h > 0$, the decrease in the susceptible population ratio due to the spread of infection has a larger negative effect on the rate of change in the number of newly infected people as the infection spreads.

An increase in the vaccination rate is also expected to cause a decrease in the susceptible population ratio. The variable for the vaccination rate, $\tilde{\nu}_{it}^h$, is defined by the number of people who completed the second vaccination in week t, V_{it}, and the efficacy of the vaccine, σ, as follows:

$$\tilde{\nu}_{it}^{h} = h \log\left(1 - \sigma \frac{\sum_{j=0}^{t-2} V_{ij}}{N}\right) = h \log(1 - \sigma \nu_{i,t-2}).$$

Note that we use the cumulative value up to two periods before taking into account the fact that it takes two weeks for a sufficient infection prevention effect to appear and set the efficacy rate to $\sigma = 0.895$. Therefore, the interpretation of the sign of the coefficient λ^h is the same as that of the variable for cumulative infected persons.

3 Data

In this section, we describe the data used in the analysis. First, for the number of newly infected persons, we use the daily data by prefecture obtained from the open data of "Trend in the number of newly confirmed cases (daily)" in the section "Visualizing the data: information on COVID-19 infections" on the website of the Ministry of Health, Labor and Welfare (MHLW).[*15] According to the remarks on the site, "The number of newly confirmed cases is calculated based on the HER-SYS data. Of note, during the period of 14 days from the most recent updated date, the number of newly confirmed cases is calculated by summing the number of cases published via press release by each jurisdiction, including cases with recurrent positive tests." The number of infected people tends to show a strong weekly effect; hence, we use the weekly total (weekly total of the number of positive cases by day), which covers the period from Sunday to Saturday, for the following empirical analysis.

Although the number of new positive cases since January 16th, 2020, is available on the website, in many prefectures, the number of weekly observations was zero before the second wave of infection. Therefore, our beginning of the analysis period is set as July 5th, 2020, when the infection had spread nationwide, and many prefectures had started to record at least one total positive case per week. The analysis is conducted in

[*15] URL is: https://covid19.mhlw.go.jp/?lang=ja/. The data acquisition date: February 2, 2022.

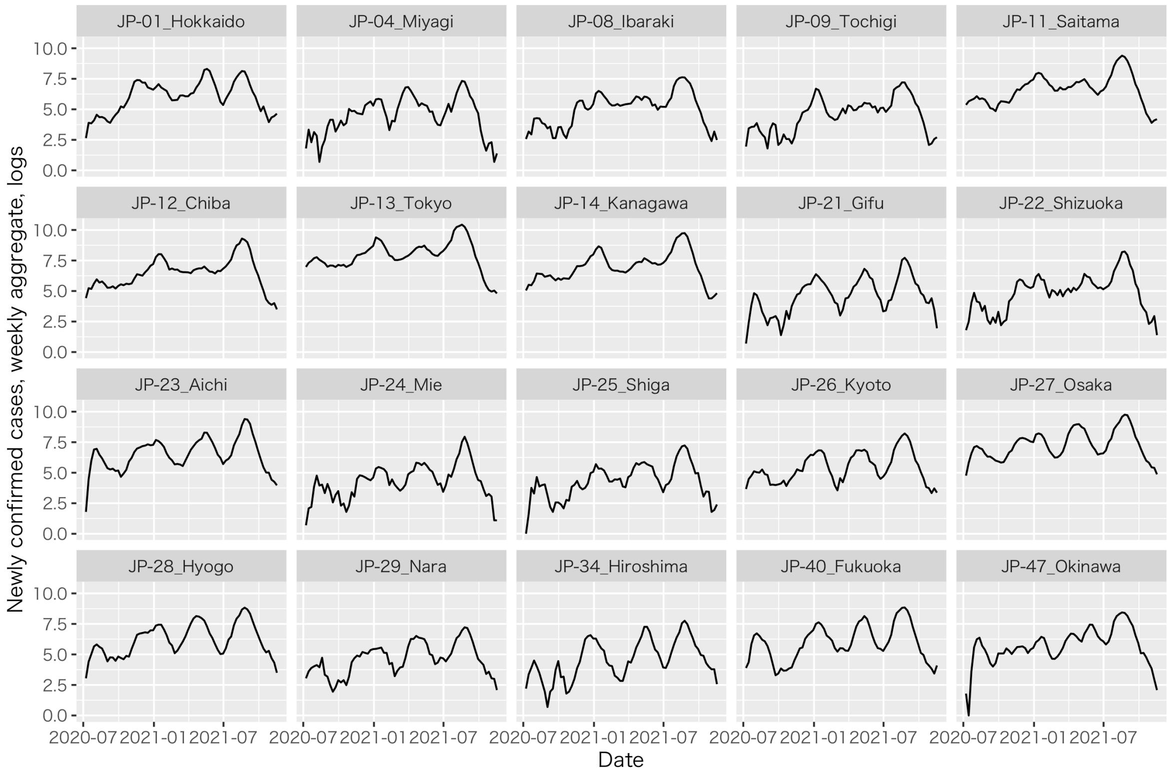

Fig. 1 Number of new infections per week (in logarithm)

Note: From the “Trend in the number of newly confirmed cases (daily)” open data available on the Ministry of Health, Labour and Welfare website *Visualizing the data: information on COVID-19 infections* author’s calculation. The period shown in the figure is from the week of July 5th, 2020, through the week of November 14th, 2021. The figure shows the 20 prefectures, where the number of new weekly infections was at least one during the same period. The date on the horizontal axis was adjusted to the date on Wednesday for each week. For example, the first week of the sample period is from Sunday, July 5th, 2020, to Saturday, July 11th, 2020, but the values for this week are shown at the position of Wednesday, July 8th, 2020.

20 prefectures with a relatively large number of infected people, and the transition of the number of newly infected (positive) people in each prefecture is shown in Figure 1.[*16] During this period, more than one new case of infection was reported every week in these 20 prefectures; thus, the sample covered approximately 90% of the total number of infected people in Japan.[*17]

[*16] Specifically, the 20 prefectures are Tokyo, Osaka, Kanagawa, Saitama, Aichi, Chiba, Hyogo, Fukuoka, Hokkaido, Okinawa, Kyoto, Shizuoka, Ibaraki, Hiroshima, Gifu, Miyagi, Nara, Tochigi, Mie, and Shiga.

[*17] As of November 23, 2021, the number of infected people in these 20 prefectures is 1,542,665 against the total number of infected people of 1,720,509, which is 89.7% of the total number of infected people in Japan.

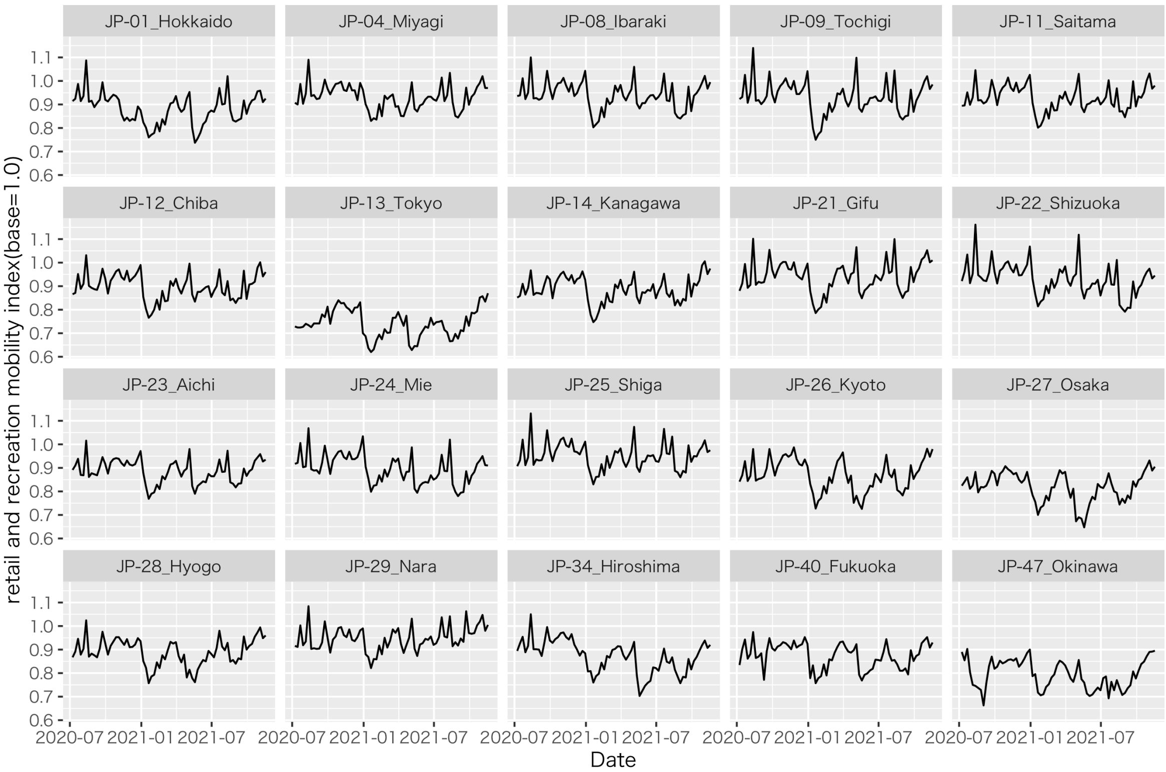

Fig. 2 Retail and recreation mobility index

Note: Authors' calculation based on the indexes given by Google COVID-19 Community Mobility Reports. The period in the figure is from the week of July 5th, 2020, through the week of November 14th, 2021, with the dates on the horizontal axis adjusted to the Wednesday of each week.

For mobility data, we use the indexes by prefecture and category published by Google COVID-19 Community Mobility Reports.*18 The index classifies the places people visit into six categories: retail and recreation, grocery and pharmacy, parks, transit stations, workplaces, and residential. The five-week period from January 3rd, 2020, through February 6th, 2020, which is the initial period of COVID-19 infection, was used as the reference period, and the percentage increase or decrease (%) of the median day of the week during these five weeks was calculated for each day thereafter. The variables used in the estimation in the next section are first calculated as the weekly rate of change from the simple average of daily values, transformed into levels,

*18 Source: Google LLC "Google COVID-19 Community Mobility Reports". URL is: https://www.google.com/covid19/mobility/ Accessed:2021/11/25.

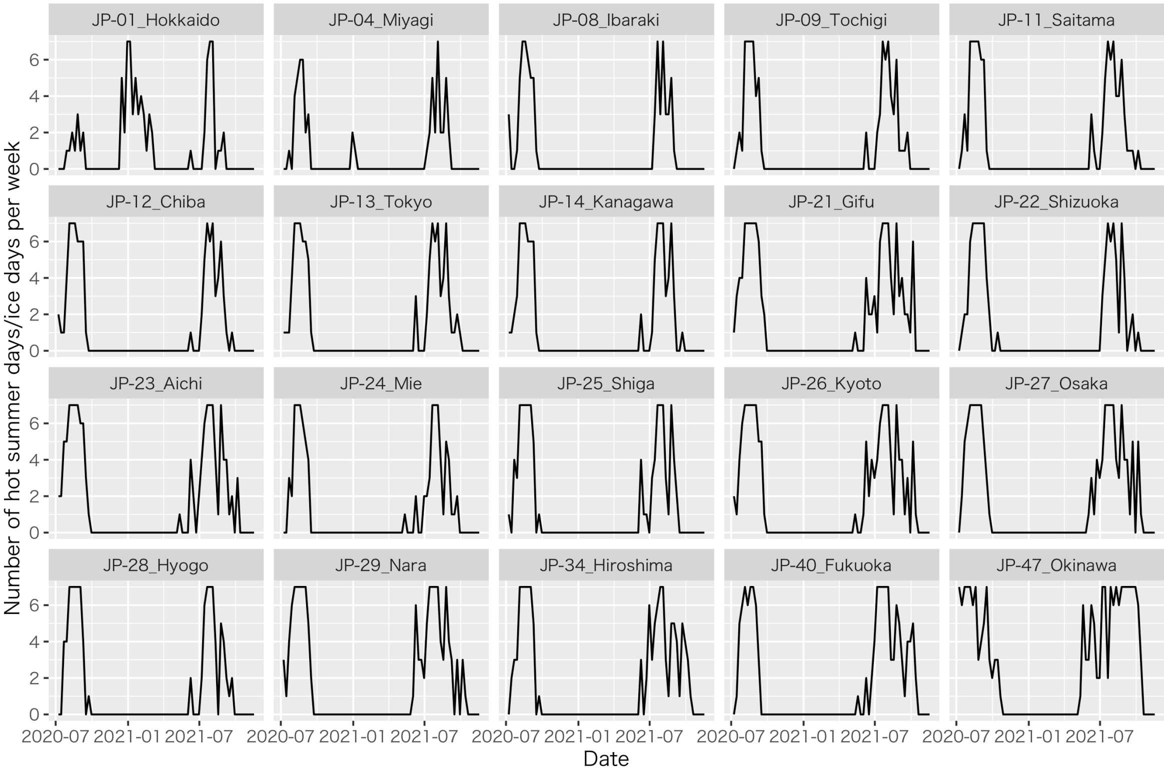

Fig. 3 The number of hot summer days and ice days per week

Note: Based on the daily maximum temperatures observed in prefectural capital from JMA data. The period depicted by the figure is the week from July 5th, 2020, through the week of November 14th, 2021, and the date on the horizontal axis is adjusted to the Wednesday of each week.

and then logarithmically transformed as shown below:

$$m = \log\left(1 + \frac{\text{average weekly rate of change}(\%)}{100}\right). \tag{6}$$

Figure 2 shows one of the six indices, the mobility index (before logarithmic transformation) for retail stores and recreation facilities. A common feature of all prefectures is that the level of indices is mostly below one, indicating a smaller number of mobility with respect to the reference period. One of the possible reasons for the large declines observed in Tokyo, Osaka, and Okinawa is that restrictions have been placed on the flow of people crossing prefectural borders.

For weather-related data, we use the daily maximum temperature and daily total precipitation obtained from the Download Historical Weather Data section of the JMA

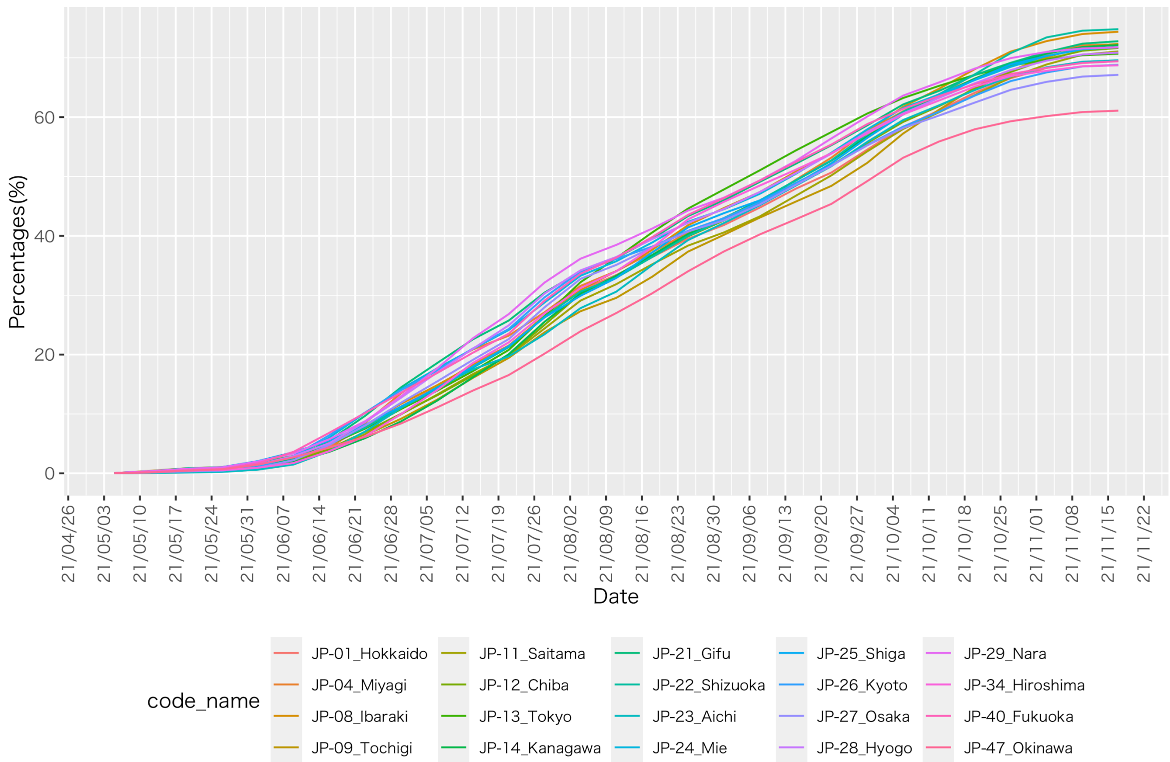

Fig. 4 Percentages of people who completed two vaccination doses

Note: Only general population vaccinations were included; values for medical personnel are not included. The period in the figure is from the week of May 2nd, 2021, through the week of November 14th, 2021, and the dates on the horizontal axis are adjusted to the Wednesday of each week.

website. Although observation data is recorded at several points in each prefecture, the data of the prefectural capital is regarded as being representative of the weather conditions for the area. Given that ventilation is most likely to be neglected because of cooling or heating on extremely hot and cold days, the number of hot summer days and ice days per week is calculated from the daily maximum temperature. We also include the weekly precipitation calculated by summing the daily precipitation as a possible weather factor, following Wilson (2021). Figure 3 shows the number of hot summer days and ice days. Since the observed values of meteorological data sometimes take zero, we use the values without logarithmic transformation in the regression analysis.

Vaccination rates are calculated using the data obtained from two sources. First, the number of weekly vaccinees by prefecture is created by aggregating the number of people who completed the second vaccination dose, based on data posted on the Government Chief Information Officers (CIOs)' Portal. The number is for general population vaccinations only, not including medical personnel.*[19] Population data by prefecture are obtained from the statistics "JUMIN KIHON DAICHO (2021)," posted on the website of the Ministry of Internal Affairs and Communications. As of October 2021, both Pfizer's vaccine and Takeda/Moderna's vaccine are available for people aged 12 years and older, but the vaccination rate is calculated as a percentage of the total population.*[20] Figure 4 shows how vaccination status progressed at about the same pace nationwide during the last six months.

The SOE declaration dummy is created by referring to the "Report on the implementation of the declaration of an SOE for the novel Coronavirus infection (October 8th, 2021)" posted on the website of "Office for the Promotion of Countermeasures against Novel Coronavirus Infections," Cabinet Secretariat.*[21] The variable takes one for weeks when an SOE is declared, and zero for other weeks. Figure 5 shows that the circumstances under which the declaration was implemented differed by region and period. The Focused Anti-infection Measures (FAM) were also being implemented as a policy to control the human mobility. However, under the SOE declaration, restaurants can be ordered or requested to close or shorten their business hours, while under the FAM, they cannot be ordered or requested to close, but only to shorten their business hours. In addition, while the declaration of an SOE covers whole prefectures, the FAMs are aimed at controlling the infection within a specific area and only cover areas designated by the governor. For this reason, the period during which the FAMs were implemented is not specifically considered in the current study.

*[19] URL is: https://cio.go.jp/c19vaccine_opendata
*[20] URL is: https://www.cov19-vaccine.mhlw.go.jp/qa/0044.html
*[21] URL is: https://corona.go.jp

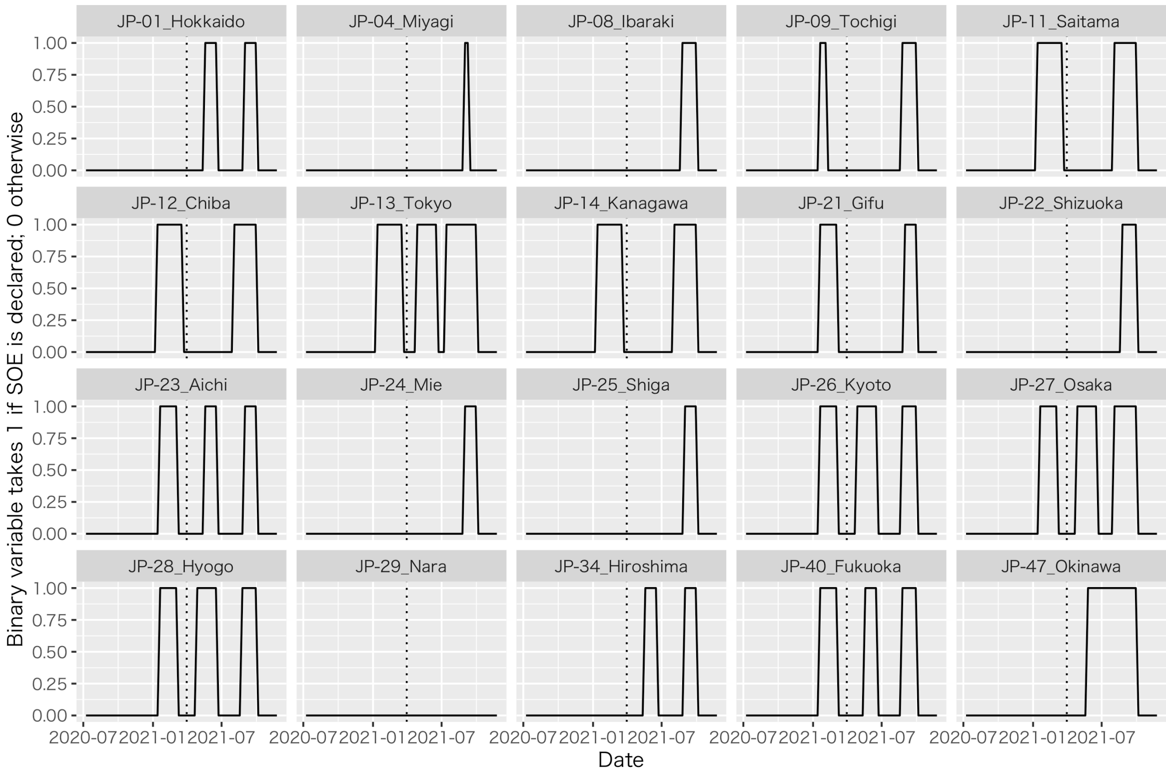

Fig. 5 Places and periods that an SOE was declared

Note: The period depicted in the figure is from the week of July 5th, 2020, through the week of November 14th, 2021, and the dates on the horizontal axis are adjusted to the Wednesday of each week. The dotted line indicates March 31, 2021.

4 Estimation results for the benchmark model

In this section, we present the estimation results of the benchmark model, Eq.(5). As already mentioned, because the local projection method is applied for impulse response analysis, Eq.(5) is estimated for different forecast horizons ($h = 1, \ldots, 5$). Since Eq.(5) is a model that includes prefectural dummies and weekly dummies, the two-way fixed effects estimator is used for estimation. The data consists of a 72-week panel covering 20 prefectures, from July 5th, 2020, through November 14th, 2021.

Controling mobility, contact opportunities, and vaccination are considered essential to control infection. The main purpose of this study is to verify this based on observational data. To this end, this study attempts to understand the dynamic relationship between the rate of change in the number of newly infected people and human mobility aggregated on a prefectural basis; however, it is necessary to devise a multifaceted understanding of mobility within a prefecture. As can be easily imagined, it is not easy to grasp the impact of mobility on a single scale because there are some locatons where mobility is locally dense and others where it is not, even within a prefecture; even if mobility increases or decreases, it may not necessarily directly lead to the spread of infection, depending on the contact opportunities. Therefore, this study analyzes the impact of increased mobility in a multidimensional manner using six different Google COVID-19 Community Mobility Reports indices.

As for the mobility and meteorological variables included in Eq.(5) and the proxies for the infection rate, there is little theoretical basis for the number of periods of time lags to be included; hence, an empirical judgement is required. Therefore, considering the time lag between infection and onset, we set the maximum lag order P to three (weeks) and search for the optimal number of lags using the information criterion. Although it depends on the combination of variables included, the Akaike information criterion and the Schwarz Bayesian information criterion often select the zero lag. Therefore, for the following estimation and impulse response analysis, we only use the contemporaneous values of mobility and weather variables by setting $P = 0$.

4.1 Estimated results for four-week ahead model

Figure 6 shows the rate of change in the number of newly infected people from four weeks ago, calculated based on the weekly total of the number of newly infected people in the analyzed 20 prefectures. The analysis period is shortened by four weeks, from the week of August 2nd, 2020 (between the first and second waves) through the week of November 14th, 2021 (the convergence period of the fifth wave). As shown in Table 1, which summarizes the descriptive statistics of the variables used in the regression analysis, the maximum rate of increase was 636.8%, while the maximum rate of

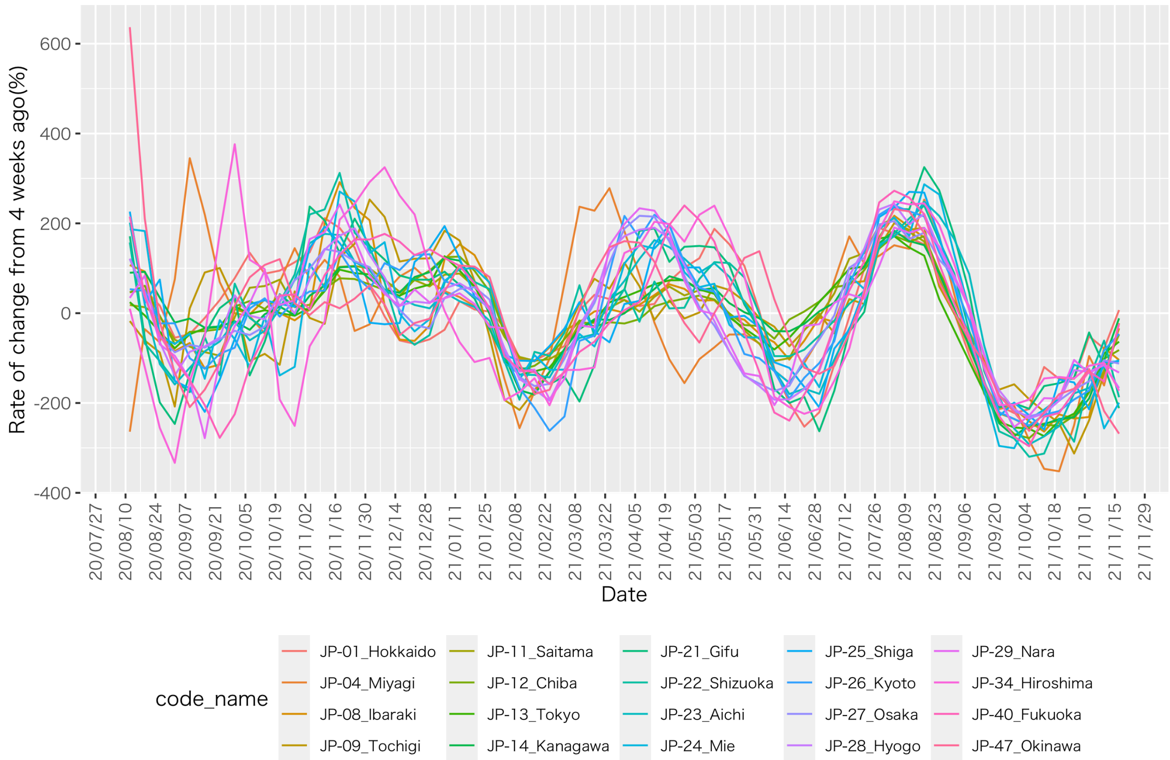

Fig. 6 Change in the number of new infections over the last 4 weeks (%): $100 \times (\log(I_t) - \log(I_{t-4}))$

Note: The period in the figure is from the week of August 2nd, 2020, to the week of November 14th, 2021, and the dates on the horizontal axis are adjusted to the Wednesday of each week.

decrease was -366.3%. In the first half of the period, differences in infected status were observed among the following regions: Hiroshima Prefecture in early December 2020, Miyagi Prefecture in March 2021, and Okinawa Prefecture at the end of May 2021 showed a marked increase. On the other hand, in the latter half of the sample period, from mid-August through mid-September 2021, the number of infected people tended to decrease rapidly nationwide.

Next, we present an overview of the estimation results and their interpretations using the model of the rate of change in the number of new infections four weeks ahead as an example. Table 2 shows the results of the prediction model Eq.(5) with $P = 0$ for the rate of change in the number of new infections four weeks ahead. Note that we allow the coefficients on SOE, $\Delta \log I$, and $\Delta \log I^*$ to be different between

Table 1 Descriptive statistics

Names of the variables	Sample size	Mean	Std. Dev.	Min.	Max.
$\log I_{t+4} - \log I_t$	1,360	−0.0338	1.3752	−3.5205	6.3682
m1 (retail & recreation)	1,440	−0.1197	0.0920	−0.4780	0.1497
m2 (grocery & pharmacy)	1,440	0.0123	0.0481	−0.1575	0.1422
m3 (parks)	1,368	−0.1041	0.1798	−0.9092	0.5686
m4 (transit stations)	1,440	−0.2954	0.1190	−0.7520	0.0862
m5 (workplaces)	1,440	−0.1549	0.1212	−0.8540	−0.0101
m6 (residential)	1,440	0.0621	0.0282	0.0114	0.1906
hot summer/ice days	1,440	1.5111	2.4409	0	7
precipitation	1,440	35.8528	53.9215	0	594
SOE dummy	1,440	0.1889	0.3916	0	1
$\Delta \log I_t$	1,420	0.0027	0.5202	−2.1401	3.6109
$\Delta \log I_t^*$	1,420	−0.0096	0.3172	−0.7226	0.8246
$4 \log(1 - c)$	1,440	−0.0197	0.0233	−0.1375	0
$4 \log(1 - \sigma\nu)$	1,440	−0.5542	1.0629	−4	0

Note: m1 to m6 are mobility indices created by the author using Eq.(6) from six indices in Google COVID-19 Community Mobility Reports. The base sample consists of 20 prefectures for 72 weeks from July 5th, 2020, through November 14th, 2021. For Shiga Prefecture, m3 (parks) was excluded because of missing values.

the period up to March 2021 and the period after April 2021 to capture a possible change in the people's behavior toward compulsory and voluntary suppressions. As can be seen from the table, the values of R^2 are approximately 0.75 for all the models, indicating this specification has high explanatory power. Of the three factors related to the infection rate, the regression coefficients for all six mobility reports indices have the expected sign and are statistically significant. As for the meteorological factors, the impact of precipitation is negligible. However, the coefficients on hot summer and ice days are positive and significant, indicating that a one day increase in the hot summer and ice days during a week would increase the infection rate by approximately 3–5% after 4 weeks. This is consistent with the expectation that infections are more likely to spread during periods of hot summer and ice days, during which there are concerns about lowered immunity due to extreme temperatures and lowered indoor ventilation due to the use of air conditioners and heaters. Finally, SOE declarations as a means of mobility controls implemented to minimize the spread of infections are confirmed to be a significant cause of reduction in new infections, only

Table 2 Benchmark model, estimated up to 72 weeks, with prefecture and weekly fixed effect dummies, four weeks ahead

	Google COVID-19 Community Mobility Reports					
	(1) retail & recreation	(2) grocery & pharmacy	(3) parks	(4) transit stations	(5) workplaces	(6) residential
mobility	5.726^{***}	4.177^{***}	1.334^{***}	3.349^{***}	2.487	-26.264^{***}
	(0.950)	(1.547)	(0.273)	(0.514)	(1.537)	(4.772)
hot summer/ice days	0.038^{*}	0.029	0.053^{**}	0.039^{*}	0.027	0.050^{**}
	(0.021)	(0.022)	(0.023)	(0.020)	(0.021)	(0.023)
precipitation	0.001	0.00001	0.001	0.001	−0.0004	0.001^{*}
	(0.001)	(0.001)	(0.001)	(0.001)	(0.001)	(0.001)
SOE(-2021/3)	-0.181^{**}	-0.516^{***}	-0.557^{***}	-0.374^{***}	-0.448^{***}	-0.186^{**}
	(0.076)	(0.068)	(0.070)	(0.065)	(0.081)	(0.082)
SOE(2021/4-)	0.188^{*}	−0.080	−0.053	0.068	−0.104	0.080
	(0.110)	(0.089)	(0.091)	(0.098)	(0.098)	(0.107)
$\Delta \log I$(-2021/3)	-0.303^{***}	-0.296^{**}	-0.292^{**}	-0.315^{***}	-0.299^{**}	-0.316^{***}
	(0.110)	(0.116)	(0.134)	(0.109)	(0.119)	(0.110)
$\Delta \log I$(2021/4-)	-0.325^{**}	-0.345^{**}	-0.420^{**}	-0.316^{**}	-0.356^{**}	-0.343^{**}
	(0.136)	(0.147)	(0.174)	(0.129)	(0.148)	(0.135)
$\Delta \log I^*$(-2021/3)	-4.220^{**}	-5.589^{***}	-5.143^{***}	-4.422^{***}	-5.610^{***}	-4.470^{***}
	(1.698)	(1.648)	(1.744)	(1.569)	(1.673)	(1.570)
$\Delta \log I^*$(2021/4-)	−4.805	-6.799^{**}	-7.443^{**}	-6.015^{*}	-6.794^{**}	-6.873^{**}
	(3.324)	(3.297)	(3.420)	(3.316)	(3.160)	(3.283)
$4\log(1-c)$	6.615^{***}	3.784	4.229^{*}	5.853^{**}	3.671	2.505
	(2.556)	(2.342)	(2.565)	(2.329)	(2.457)	(2.354)
$4\log(1-\sigma\nu)$	-0.450^{*}	-0.598^{**}	-0.804^{***}	-0.507^{*}	-0.629^{**}	-0.527^{**}
	(0.260)	(0.261)	(0.249)	(0.266)	(0.256)	(0.250)
Observations	1,340	1,340	1,273	1,340	1,340	1,340
R^2	0.761	0.749	0.751	0.761	0.748	0.761

$^{*}p<0.1$; $^{**}p<0.05$; $^{***}p<0.01$

Note: Figures in parentheses are heteroskedasticity-consistent standard errors by Arellano (1987), which are clustered by time and consider correlations among prefectures.

during the first sub-sample period. Regarding the coefficients on the rate of change in the number of new infections in the previous week, they are all negative, and are statistically significant for both sub-sample periods. It can be interpreted as capturing the tendency of decreasing new infections over the next four weeks as a precaution against the further spread in a situation wherein the infection is actively spreading. Differences in the coefficients, along with the coefficients on SOE, between two sub-samples will be further examined in the next subsection.

Next are the results for factors related to the susceptible population. The coefficient on the cumulative infected population is positive as expected, but in many cases, not significant. This implies that an increase in the number of cumulative infected people

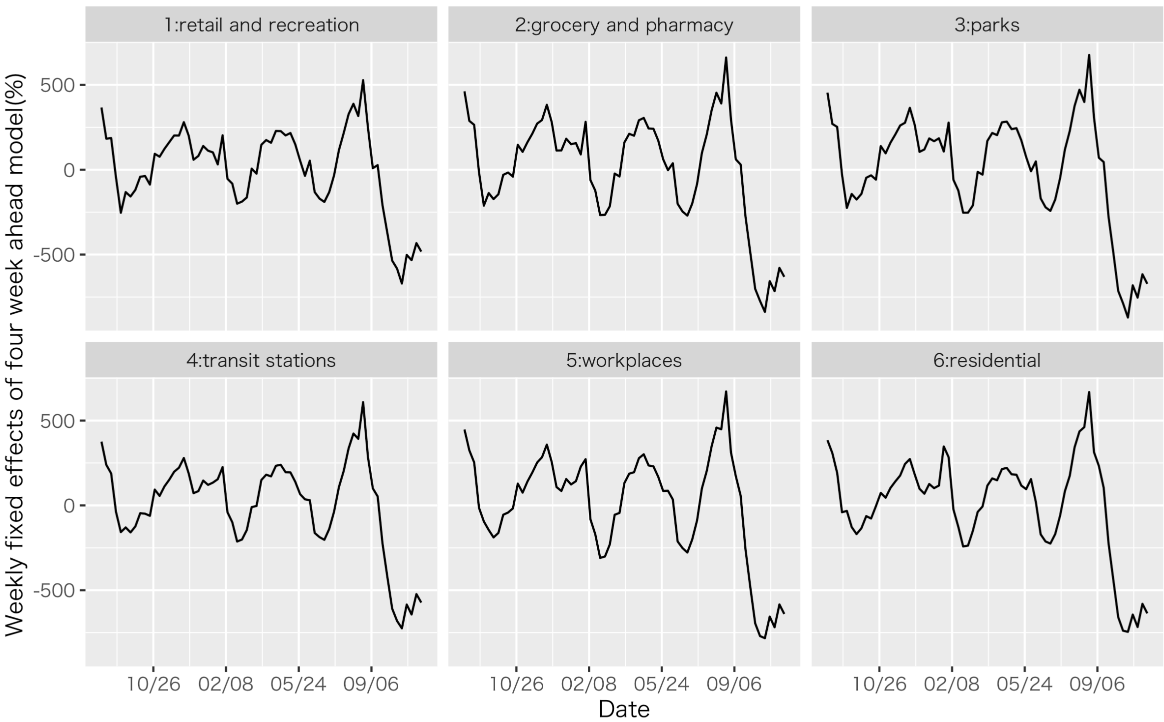

Fig. 7 Estimates of weekly time fixed effect, $\hat{\alpha}_t^4$

Note: The estimates are adjusted such that the mean value is zero. The date on the horizontal axis is the week being forecasted, not the week when the forecast is made. Also, the dates on the horizontal axis are adjusted to the Wednesday of each week. For example, the first week of the sample period is from Sunday, August 2nd, 2020, through Saturday, August 8th, 2020, but the values for this week are shown at the position of Wednesday, August 5th, 2020.

in the past decreases the susceptible population, resulting in a decrease in the number of newly infected people. However, since the ratio of cumulative infected people in Japan is extremely low compared to other countries, it is understandable that this coefficient, which represents the effect of mass immunization, is not significant for many cases. On the other hand, for the coefficients on vaccination, all signs are in the opposite direction to that expected and are significant in all the models. This may suggest that the current model is mis-specified. Therefore, the effect of vaccination will be re-examined later by adding another perspective.

Finally, we investigate the estimates of weekly time fixed effects. Figure 7 shows the transition of the time fixed effects estimated from the four-week ahead model for each of the six indicators. The date on the horizontal axis is not the week being forecasted, but the Wednesday of the four weeks ahead. Figure 7 shows that although the number of periods with positive values increased throughout the sample period, there was a sharp decline after September 2021. In other words, the sharp decline in the number of infected people after September 2021 cannot be completely explained by variables such as mobility, weather, and vaccination. In addition, the spikes commonly observed around the end of January 2021 in all graphs suggest that there are factors that increased the spread of infection from the end of the year to the end of January, which cannot be fully explained by changes in the explanatory variables included in the model, such as family gatherings during New Year holidays.[*22]

In addition, the six images in Figure 7 show a common increase in the value of time dummies from the beginning of February to the end of March 2021 and from the beginning of June to the beginning of August 2021. Although it is difficult to identify the cause of the increase, this period also coincides with the period when the ratio of conventional to mutant species is believed to have increased. For the period of June through August, according to the National Institute of Infectious Diseases' Infectious Agents Surveillance Report (IASR, November 2021), "the Delta variant was first detected in quarantine in late March 2021. After domestic infected cases were confirmed in April, they were rapidly replaced. By the end of August, about 90% of the cases whose genomes had been sequenced in metropolitan areas were delta variants."[*23] Since the model in this study did not include variables that represented the emergence of variant strains or changes in viral characteristics, it can be inferred that the weekly dummy captures this type of factor.

[*22] For example, Hiroshi Nishiura, a professor at Kyoto University, said, "We saw a tendency for the 'effective reproduction number,' an indicator of how many people can be infected by one person, to rise when there are consecutive holidays, and it rose even during the declaration of the SOE." (URL is: https://www3.nhk.or.jp/news/html/20211006/k10013294851000.html, 2021/10/6, Accessed: 2021/12/15)

[*23] URL is: https://www.niid.go.jp/niid/ja/2019-ncov/2502-idsc/iasr-in/10796-501c03.html.

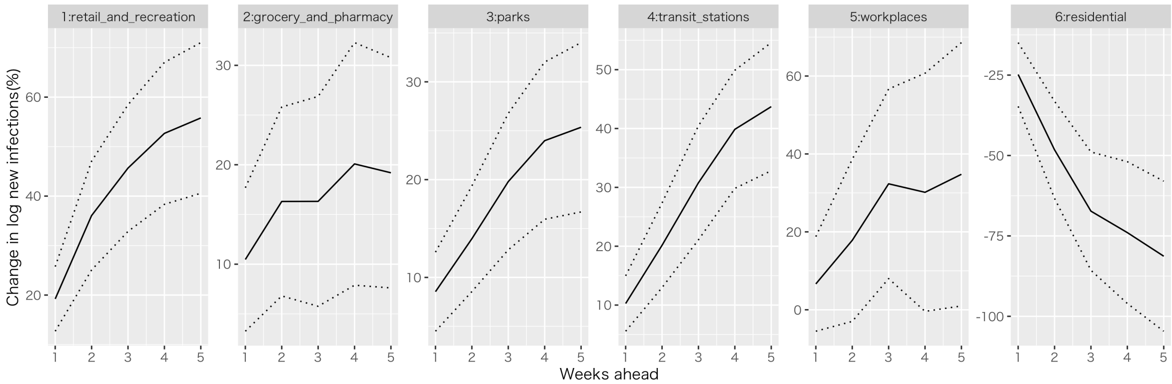

Fig. 8 IRFs of the rate of change in the number of newly infected persons to a one standard deviation increase in mobility

Note: The solid lines correspond to the point estimate, and the dotted lines correspond to 90% confidence interval.

4.2 Impulse Response Analysis

Further, based on the local projection method, we conduct an impulse response analysis of the response of the rate of change in the number of newly infected people to changes in mobility. Figure 8 shows the impulse response functions (IRFs) of the rate of change in the number of new infections when the six mobility indices increase by one standard deviation (hereafter referred to as a one standard deviation increase in mobility).*24 As mentioned above, one week is considered as one period in this analysis; hence, the first scale on the horizontal axis of the graph in Figure 8 represents one week. The impulse response and its 90% confidence interval are calculated from the coefficient β^h ($h = 1, \ldots, 5$) and its time-clustered heteroskedasticity-robust standard error (Arellano (1987)) estimated by the panel OLS based on Eq.(5). It shows the percentage change in the number of new infections due to a one standard deviation increase in mobility over the originally expected level.

As can be seen from Figure 8, for the five indices except for residential index, a one

*24 As shown in Table 1, the standard deviation of the mobility index is 9.20% for retail and recreation, 4.81% for grocery and pharmacies, 17.98% for parks, 11.9% for transit stations, 12.12% for workplaces, and 2.82% for residential.

standard deviation increase in mobility is found to significantly increase the rate of change in the number of new cases over the next five weeks. For example, for the retail and recreation index, the results indicate that the average increase is monotonically increasing from 20% after one week to 55% after five weeks.

As for the increase in mobility related to transit stations and workplaces, the additional increase in the number of newly infected people is over 30% after three to four weeks. This result is interesting because it suggests that remote work—a form of work style that is becoming more widespread because of the COVID-19-induced work style reform—has the effect of suppressing infection by reducing mobilities related to transit stations and workplaces while maintaining economic activity. In addition, for the residential index, which is believed to have increased due to remote work, it is noteworthy that the increase in the residential mobility contributes to curbing the spread of infection and that the magnitude of the change is also larger than that of other indicators (a decrease of approximately 80% for a one standard deviation increase). The increase in the number of people visiting parks raises the infection growth rates by approximately 25% in five weeks. Finally, the increase in the number of people visiting grocery stores and pharmacies contributes to the spread of infection, but its confidence interval is very wide, and its impact is smaller than that of other mobilities.

Next, Figure 9 illustrates the effects of a one-day increase in hot summer and ice days per week, which increase infection by approximately 3–6% after three weeks for all indices. As shown in Figure 3, in summer and winter, it is possible to have several weeks of hot summer or ice days; hence, these results also suggest that the cumulative effects of extreme temperatures can be considerable and proper ventilation as well as countermeasures to maintain resistence are effective in helping to control infection.

Finally, we compare the "intervention effect" on deterring infections by declaring

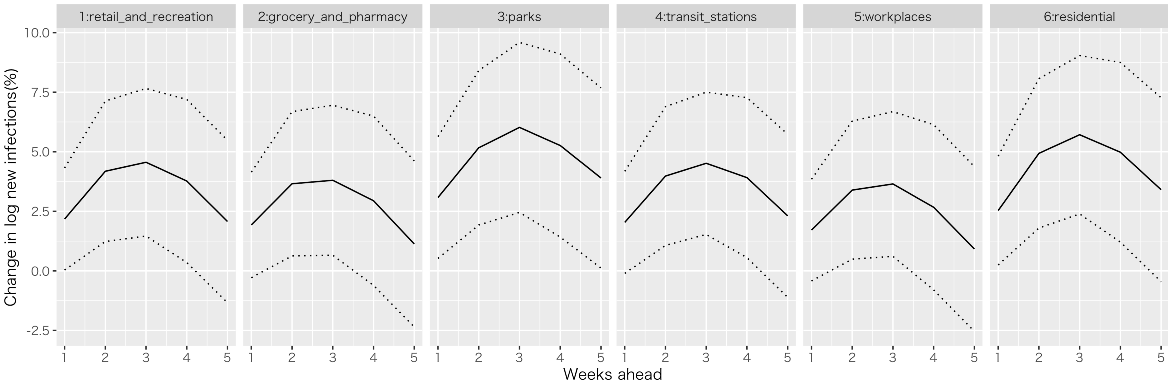

Fig. 9 IRFs of the rate of change in the number of new infections in response to a one-day increase in the number of hot summer and ice days

Note: The solid lines correspond to the point estimate, and the dotted lines correspond to 90% confidence interval.

the SOEs to regulate mobility with that of "information effect," which is expected to induce voluntary restraint. As can be seen, the left half of Figure 10 shows that although the degree of the suppression effect varies depending on the type of mobility index, the effect of reducing the rate of increase in the number of new infections is significant for all indices during the first sub-sample period. For the indices of grocery stores/pharmacies and parks, the average reduction rate after five weeks is over 50%, and for the indices of public transportation and workplaces, it is about 40%. These results clearly indicate that this policy had a distinct effect on controlling infection in the early stage of declaration. However, for the latter half of the sample period, the results show little significant suppression effect for all indices and all forecast horizons except for five weeks horizon. For a five weeks horizon, the SOE declaration appears to have some negative effects for some cases, but the magnitude is less than half compared with the first sub-sample period. These results indicate that the effectiveness of the SOE intervention effect only exists in the first half of the sample period and is limited in the second sample period.

On the other hand, the right half of Figure 10 shows the IRFs of the infection

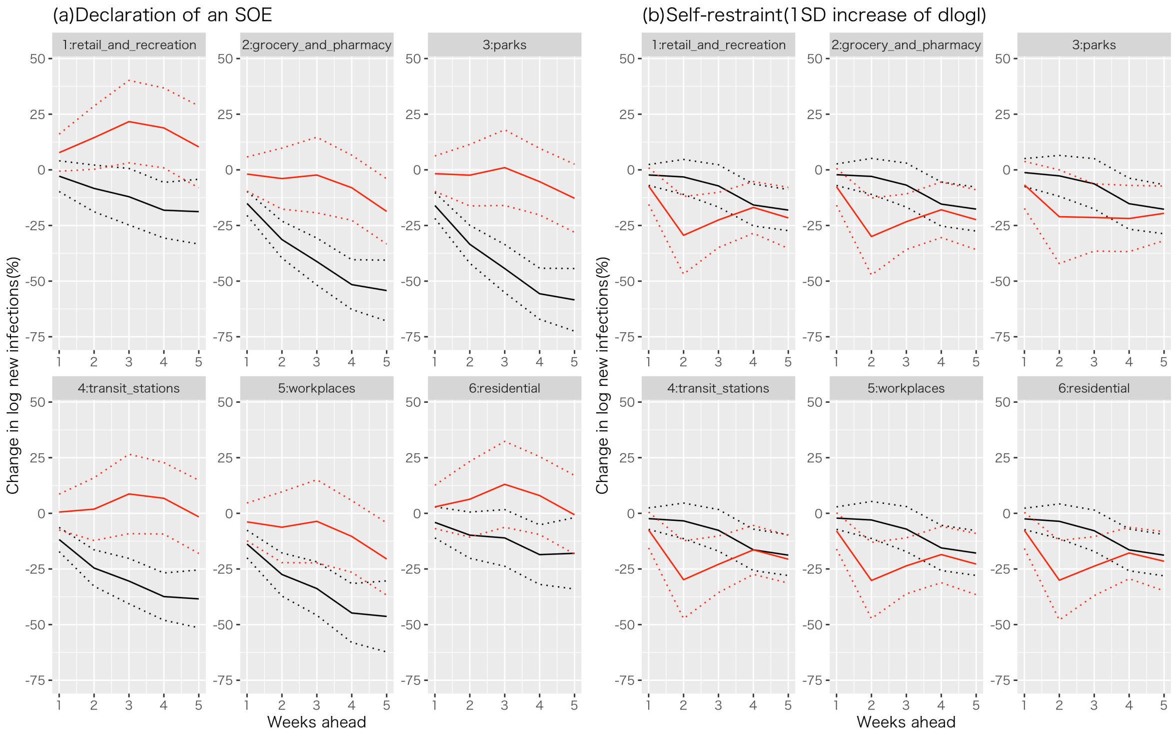

Fig. 10 Declaration of an SOE vs. self-restraint (including the situation nationwide)

Note: The solid lines correspond to the point estimate, and the dotted lines correspond to 90% confidence interval. The responses colored in black are calculated from the parameters of the first sub-sample period (before March 2021), and those in red are from the second sub-sample period (after April 2021).

growth rates to a one-standard deviation increase in the infection growth rate in the last week (information effect). The unanticipated recent deterioration of the infection situation, a possible measure of "fear", tends to reduce the number of infected people in both the first and second sub-samples. Furthermore, while it takes four weeks for a significant reduction to emerge in the first half of the sample, a statistically significant reduction of more than 20% is observed in the second half of the sample in as soon as two weeks, and the effects persist albeit with a wider confidence interval.

5 Analysis of Vaccination Effectiveness

Was vaccination ineffective in controlling the infection? According to the SIR model, there are two possible pathways through which vaccination may affect the rate of new infections. First, vaccination may reduce the susceptible population and thus reduce the rate of change in the number of new infections. However, the results of the previous section could not find any evidence of the effect of vaccination on the reduction of the rate of change in the number of new infections through the reduction of susceptible population. Another potential channel is the possibility that vaccination may inhibit the spread of infection through mobility. In other words, if vaccination is an effective means of preventing infection, it would be expected that an increase in mobility by the same amount would not result in the same spread of infection during periods of increased vaccination rates rather than during unvaccinated periods. Since this possibility was not considered in the benchmark model in the previous section, we extend the model in this section to examine this possibility as follows.[*25]

$$\begin{aligned}\log I_{i,t+h} - \log I_{it} = \psi^h m_{it} + \kappa^h m_{it}\tilde{\nu}_{it}^h + \delta^h w_{it} + \phi^h SOE_{it} + \rho^h \Delta \log I_{it} \\ + \rho^{*h} \Delta \log I_{it}^* + \theta^h \tilde{c}_{it}^h + \lambda^h \tilde{\nu}_{it}^h + \alpha_t^h + \alpha_i^h + \epsilon_{i,t,t+h}\end{aligned} \tag{7}$$

This model adds an interaction term between the vaccination rate $\tilde{\nu}_{it}^h$ and the mobility index m_{it} to Eq.(5). As a result, the impulse response of the rate of change in the number of newly infected people to a 1% increase in mobility due to an increase in the vaccination rate changes, as shown in the following equation:

$$\frac{\partial(\log I_{i,t+h} - \log I_{it})}{\partial m_{it}} = \psi^h + \kappa^h \tilde{\nu}_{it}^h \tag{8}$$

As shown in Eq.(8), in this model, the impulse response of the rate of change of the number of newly infected people to the mobility depends on the vaccination rate. If the vaccination rate is 0%, the second term is zero, and the impulse response coefficient is ψ^h, which is identical to the benchmark model. However, when the vaccination rate takes a positive value, $\tilde{\nu}_{it}^h$ will take a negative value. Therefore, if κ^h

[*25] As in the analysis procedure of the previous section, we first searched for the optimal lag length for m_{it} and w_{it} based on two information criteria, but both criteria suggested zero as the optimal lag order. Hence the only current variables are included.

Table 3 Models with cross-product term, estimated up to 72 weeks, with prefecture and weekly fixed effect dummies, four weeks ahead

	Google COVID-19 Community Mobility Reports					
	(1)	(2)	(3)	(4)	(5)	(6)
	retail & recreation	grocery & pharmacy	parks	transit stations	workplaces	residential
mobility	5.996^{***}	4.767^{***}	1.547^{***}	3.473^{***}	2.489	-26.151^{***}
	(1.031)	(1.628)	(0.278)	(0.534)	(1.607)	(4.830)
$4\log(1-\sigma\nu)$	0.843^{*}	1.315^{*}	0.541^{**}	0.385	0.006	0.501
$\times$ mobility	(0.442)	(0.720)	(0.241)	(0.330)	(1.096)	(2.933)
hot summer/ice days	0.038^{*}	0.029	0.053^{**}	0.039^{*}	0.027	0.049^{**}
	(0.021)	(0.021)	(0.023)	(0.021)	(0.022)	(0.024)
precipitation	0.001	0.00001	0.001	0.001	−0.0004	0.001^{*}
	(0.001)	(0.001)	(0.001)	(0.001)	(0.001)	(0.001)
SOE(-2021/3)	-0.143^{*}	-0.508^{***}	-0.541^{***}	-0.362^{***}	-0.448^{***}	-0.190^{**}
	(0.081)	(0.067)	(0.069)	(0.065)	(0.089)	(0.086)
SOE(2021/4-)	0.148	−0.069	−0.048	0.046	−0.104	0.083
	(0.099)	(0.089)	(0.087)	(0.098)	(0.098)	(0.114)
$\Delta \log I$(-2021/3)	-0.304^{***}	-0.297^{**}	-0.296^{**}	-0.317^{***}	-0.299^{**}	-0.315^{***}
	(0.109)	(0.116)	(0.134)	(0.109)	(0.119)	(0.110)
$\Delta \log I$(2021/4-)	-0.342^{**}	-0.345^{**}	-0.447^{**}	-0.309^{**}	-0.356^{**}	-0.343^{**}
	(0.133)	(0.143)	(0.177)	(0.132)	(0.148)	(0.135)
$\Delta \log I^*$(-2021/3)	-0.041^{**}	-0.056^{***}	-0.051^{***}	-0.044^{***}	-0.056^{***}	-0.045^{***}
	(0.017)	(0.016)	(0.017)	(0.016)	(0.017)	(0.016)
$\Delta \log I^*$(2021/4-)	-0.056^{*}	-0.070^{**}	-0.075^{**}	-0.063^{**}	-0.068^{**}	-0.066^{**}
	(0.033)	(0.033)	(0.032)	(0.032)	(0.028)	(0.031)
$4\log(1-c)$	9.511^{***}	5.547^{*}	7.857^{***}	6.667^{**}	3.685	2.100
	(3.646)	(2.902)	(3.049)	(2.624)	(4.398)	(4.131)
$4\log(1-\sigma\nu)$	−0.251	-0.753^{***}	-0.643^{***}	−0.412	−0.627	−0.578
	(0.309)	(0.267)	(0.236)	(0.285)	(0.398)	(0.465)
Observations	1,340	1,340	1,273	1,340	1,340	1,340
R^2	0.762	0.749	0.751	0.761	0.748	0.761

*p<0.1; **p<0.05; ***p<0.01

Note: Figures in parentheses are heteroskedasticity-consistent standard errors by Arellano (1987), which are clustered by time and consider correlations among prefectures.

is positive, the model shows that the impact of mobility on the rate of change in the number of infected people decreases as the vaccination rate increases.

To see the impact of the added interaction terms, Table 3 summarizes the estimation results for the four-week-ahead infection growth rate model. The table shows that the results are qualitatively unchanged from the benchmark models, as reported in Table 2. Specifically, an increase in the mobility—excluding residential—and an increase in the number of hot summer and ice days tend to significantly increase the rate of change in the number of newly infected people. In contrast, an increase in the residential mobility, the declaration of an SOE, and the deteriation of current infection status tend to significantly decrease the rate of increase in the number of newly infected people. The coefficients of the newly-added interaction term between vaccination rates and mobility are estimated to be positive for all mobilities and significantly positive in the models for retail and recreation, grocery stores/pharmacies, and parks. This implies that the impact of mobility on the rate of change in the number of new infections declines as vaccination rates increase, suggesting that vaccination has had some effect on infection control.

Next, to investigate the possibility that the proportion of people with the second dose of vaccine might reduce the spread of infection by mobility, we calculate the IRFs across the following four time points based on Eq.(7).

1. Before vaccination begins
2. August 1st, 2021 (The percentage of those who completed the second vaccination two weeks ago was 21.28%)
3. September 12th, 2021 (The percentage of those who completed the second vaccination two weeks ago was 43.32%)
4. October 24th, 2021 (The percentage of those who completed the second vaccination two weeks ago was 62.33%)

Specifically, at these time points, the number of people who had received the second dose of vaccine as of two weeks prior to the time is summed up for 20 prefectures, and it is divided by the total population of the region. The IRFs are evaluated using these percentages.

Figure 11 illustrates the IRFs evaluated at the above four time points. From the figure, mobility, except for residential, significantly increases the rate of change in the number of new infections in the period before the commencement of vaccination, as we saw in the previous section. For example, a one-standard-deviation increase in the

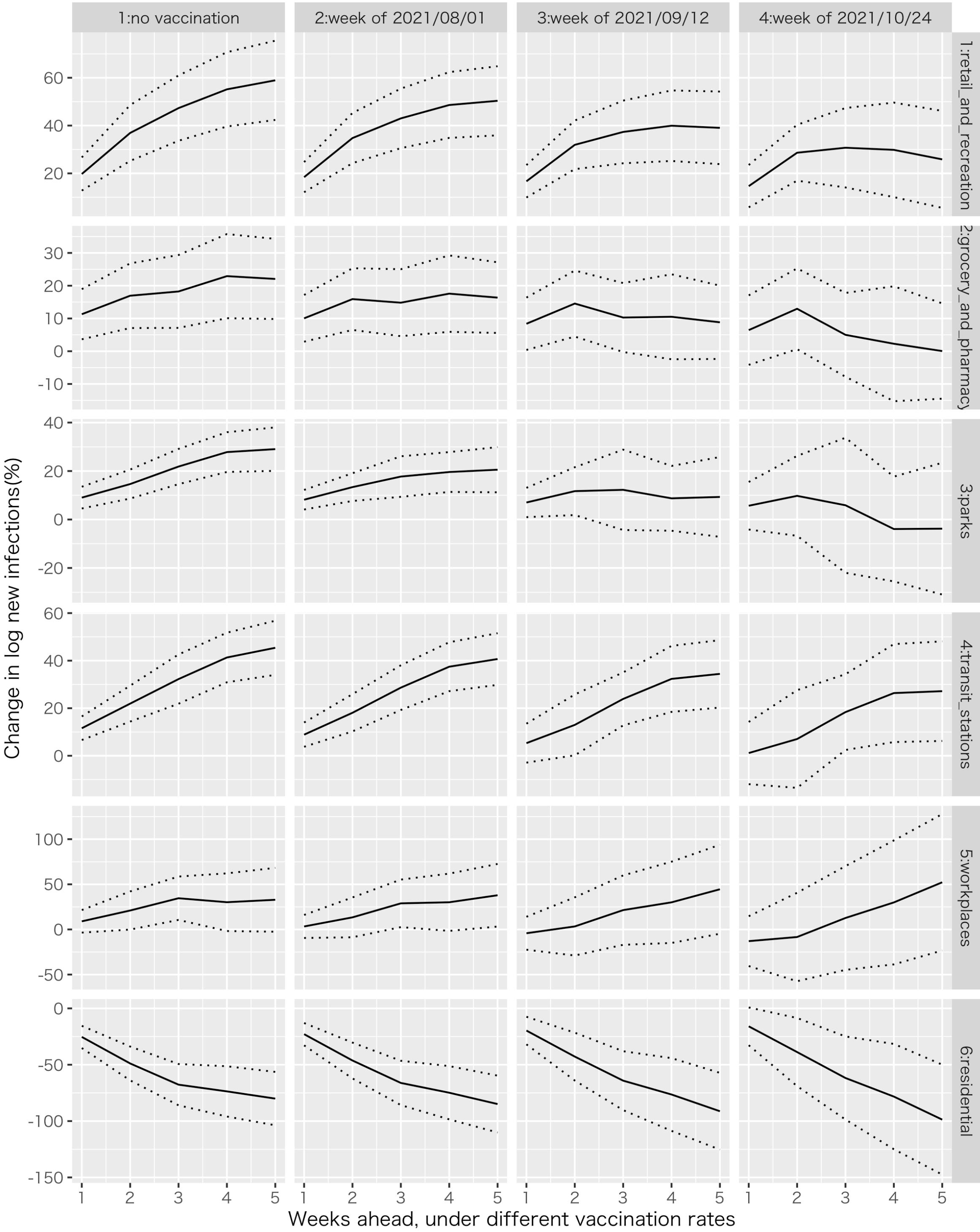

Fig. 11 IRFs of the rate of change in the number of newly infected persons to a one-standard-deviation increase in mobility under different vaccination rates

Note: The solid lines correspond to the point estimate, and the dotted lines correspond to 90% confidence interval. Vaccination rates are, from left to right: 0%, 21.28%, 43.32%, and 62.33%.

flow of people to retail stores and recreation facilities increases the rate of change in the number of newly infected people by about 37% over the next two weeks. After five weeks, the increase in the rate of change in the number of new infections reaches 58.9% on average, with a 90% confidence interval of 42.3% to 75.5%. However, Figure 11 shows that this trend gradually decreases with vaccination rates. In early August 2021, when the vaccination rate exceeded 20%, the average rate of increase over the next five weeks has dropped to 50.3% (with a 90% confidence interval of $[35.9, 64.8]$), and by September 12, when the vaccination rate reached 50%, the average rate is about 39.0%. Furthermore, in late October, when the vaccination rate exceeded 60%, the average growth rate after five-weeks further has decreased to 25.8%. Moreover, the lower bound of the 90% confidence interval has decreased to 5.5%, confirming that the relationship between the increase in mobility and the rate of change in the number of new infections has been weakening. The decreasing tendency in the effect of mobility on the rate of change in the number of new infections is also evident in grocery stores/pharmacies and parks, indicating that the average rate of spread decreases with an increase in the vaccination rate. Specifically, in mid-September, when the vaccination rate exceeded 50%, the relationship between the increase in mobility and the spread of infection in grocery stores, pharmacies, and parks has become significant only in the short term, and by late October, it has become insignificant. In addition, the impact of mobility in transit stations on the rate of change in the number of new infections has also declined significantly, and the short-term relationship between the two has become completely insignificant by the end of October. Furthermore, the impact of workplace mobility on the rate of change in the number of new infections has decreased significantly.

6 Conclusion

In this study, we used the SIR model to analyze the dynamic relationship between the mobility and the rate of change in the number of newly infected people, and the impact of the vaccine on this relationship, in order to examine the effectiveness of the SOE and vaccination in controlling the transmission of COVID-19. The analysis confirmed that the declaration of an SOE had a significant effect on reducing the rate of change in the number of new infections. However, the effect was observed only in the early stages of implementation, and its effect has been almost disappeared in the recent period. On the other hand, the effect of self-restraint in reducing the spread of infection was observed in both periods. In addition, it was confirmed that mobility in all categories of locations other than residential mobility significantly increased the rate of change in the number of new infections. Although it has been noted that there is a positive relationship between mobility in retail stores, recreation facilities, and workplaces and the rate of change in the number of new infections, the quantitative evaluation of this relationship based on actual data is a major contribution of this study. In addition, our results suggested that the rate of change in the number of new infections tended to decrease significantly when residential mobility increased. The result indicated that staying at home can reduce infection and showed the effectiveness of using such policies promoting remote work and regulating restaurants and businesses. Although the effectiveness of these policies was expected, it is meaningful that we were able to provide a quantitative evaluation of their effectiveness.

This study also provided valuable insight regarding the effectiveness of the administration of vaccination: The results did not show a significant infection control effect through reducing the susceptible population; however, there was a significant reduction in the positive relationship between mobility and the rate of change in the number of new infections. In particular, the reduction effect was greater in retail stores and recreation facilities, grocery stores, pharmacies, and parks. These results provided a certain basis for economic revitalization policies as the number of people vaccinated increases and will be of great assistance in implementing economic revitalization policies.

This study is one of few that analyzed the dynamic relationship between mobility and the rate of change in the number of new infections from actual, observable data. Therefore, the results obtained are highly relevant; at the same time, it should be noted that there are some major limitations. First, we used the Google COVID-19 Community Mobility Reports index for six different locations as the data for mobility; however, the appropriateness of this index—as a measure of mobility in each prefecture—is a matter of debate. The index does not distinguish between inter-prefectural travel, and the model does not explicitly consider the possibility of virus transmission from neighboring prefectures; hence, there is little to suggest that inter-prefectural travel played a role in spreading infection. However, a quantitative evaluation of the impact of inter-prefectural travel on the spread of infection will be an important issue to be addressed in the future because self-restraint has been frequently called for inter-prefectural travels. This study also confirmed that there is a large variation in the time fixed effects that cannot be explained by mobility, weather, or vaccines. This indicates that the emergence of mutant strains and changes in the nature of the virus play a major role in the increase or decrease in the number of newly infected people, suggesting that even if the relationship between mobility and the spread of infection is weakened by the increase in vaccination rates, careful attention must be paid to the emergence of mutant strains. In this sense, the Japanese government's response to the Omicron strain is understandable from the perspective of risk control. Finally, it should be noted that the data analyzed in this study comprises the number of newly infected people. A commonly-held view is that mitigating the number of serious illnesses and deaths is more important when enforcing policies, and it is interesting to analyze the relationship between mobility and vaccination rates and the number of serious illnesses and deaths from actual data. In Japan, however, the number of serious illnesses and deaths has remained low, which makes such analysis difficult. The analysis of the number of serious illnesses and deaths itself is very meaningful; however, we hope that the situation will be resolved, and there will be no need to analyze it further.

References

Allcott, H., Boxell, L., Conway, J. C., Ferguson, B. A., Gentzkow, M., and Goldman, B. (2020). What explains temporal and geographic variation in the early US coronavirus pandemic? *NBER Working Paper*, 27965.

Arellano, M. (1987). Computing robust standard errors for within group estimators. *Oxford Bulletin of Economics and Statistics*, 49(4):431–434.

Arias, J. E., Fernàndez-Villaverde, J., Ramírez, J. R., and Shin, M. (2021). Bayesian estimation of epidemiological models: Methods, causality, and policy trade-offs. *NBER Working Paper*, 28617.

Avery, C., Bossert, W., Clark, A., Ellison, G., and Ellison, S. F. (2020). An economist's guide to epidemiology models of infectious disease. *Journal of Economic Perspectives*, 34(4):79–104.

Badr, H. S., Du, H., Marshall, M., Dong, E., Squire, M. M., and Gardner, L. M. (2020). Association between mobility patterns and covid-19 transmission in the usa: a mathematical modelling study. *The Lancet Infectious Diseases*, 20(11):1247–1254.

Bisin, A. and Moro, A. (2021). JUE insight: Learning epidemiology by doing: The empirical implications of a spatial-sir model with behavioral responses. *Forthcoming in Journal of Urban Economics*, page 103368.

Brodeur, A., Gray, D., Islam, A., and Bhuiyan, S. (2021). A literature review of the economics of COVID-19. *Journal of Economic Surveys*, 35:1007–1044.

Caselli, F., Grigoli, F., Sandri, D., and Spilimbergo, A. (2021). Mobility under the COVID-19 pandemic: Asymmetric effects across gender and age. *Forthcoming in IMF Economic Review.*

Chong, Y., Jordà, O., and Taylor, A. M. (2012). The Harrod–Balassa–Samuelson hypothesis: Real exchange rates and their Long-Run equilibrium. *International*

Economic Review, 53(2):609–634.

David, A. C. and Pienknagura, S. (2021). On the effectiveness of containment measures in controlling the COVID-19 pandemic: The role of labour market characteristics and governance. *Applied Economics Letters*, 28(19):1641–1647.

Davis, S. J., Liu, D., and Sheng, X. S. (2021). Stock prices and economic activity in the time of coronavirus. *Forthcoming in IMF Economic Review.*

Eichenbaum, M. S., Rebelo, S., and Trabandt, M. (2021). The Macroeconomics of Epidemics. *The Review of Financial Studies*, 34(11):5149–5187.

Fang, H., Wang, L., and Yang, Y. (2020). Human mobility restrictions and the spread of the novel coronavirus (2019-ncov) in China. *Journal of Public Economics*, 191:104272.

Fernàndez-Villaverde, J. and Jones, C. I. (2020). Estimating and simulating a SIRD model of COVID-19 for many countries, states, and cities. *NBER Working Paper*, 27128.

Fraser, T. and Aldrich, D. P. (2021). The dual effect of social ties on COVID-19 spread in Japan. *Scientific Reports*, 11(1):1596.

Fujii, D. and Nakata, T. (2021). COVID-19 and output in Japan. *Japanese Economic Review*, 72:609–650.

Fukao, M. and Shioji, E. (2021). Is there a trade-off between COVID-19 control and economic activity? Implications from the Phillips curve debate. *Forthcoming in Asian Economic Policy Review.*

Gamtkitsulashvili, T. and Plekhanov, A. (2021). Mobility and economic activity around the world during the Covid-19 crisis. *Forthcoming in Applied Economics Letters.*

Glaeser, E. L., Gorback, C., and Redding, S. J. (2021). JUE insight: How much does COVID-19 increase with mobility? Evidence from New York and four other U.S.

cities. *Forthcoming in Journal of Urban Economics.*

Granger, C. W., Inoue, T., and Morin, N. (1997). Nonlinear stochastic trends. *Journal of Econometrics*, 81(1):65–92.

Harris, J. E. (2020). Data from the COVID-19 epidemic in Florida suggest that younger cohorts have been transmitting their infections to less socially mobile older adults. *Review of Economics of the Household*, 18:1019–1037.

Hoshi, K., Kasahara, H., Makioka, R., Suzuki, M., and Tanaka, S. (2021). Trade-off between job losses and the spread of COVID-19 in Japan. *Japanese Economic Review*, 72:683–716.

Hosono, K. (2021). Epidemic and economic consequences of voluntary and request-based lockdowns in Japan. *Journal of the Japanese and International Economies*, 61:101147.

Jordà, O. (2005). Estimation and inference of impulse responses by local projections. *American Economic Review*, 95(1):161–182.

Jung, J., Manley, J., and Shrestha, V. (2021). Coronavirus infections and deaths by poverty status: The effects of social distancing. *Journal of Economic Behavior and Organization*, 182:311–330.

Keller, G., Kersting, G., and Rösler, U. (1987). On the asymptotic behaviour of discrete time stochastic growth processes. *Annals of Probability*, 15(1):305–343.

Klebaner, F. C. (1989). Stochastic difference equations and generalized gamma distributions. *Annals of Probability*, 17(1):178–188.

Korolev, I. (2021). Identification and estimation of the SEIRD epidemic model for COVID-19. *Journal of Econometrics*, 220(1):63–85.

Kubota, S. (2021). The macroeconomics of COVID-19 exit strategy: the case of Japan. *Japanese Economic Review*, 72:651–682.

Küster, P. (1985). Asymptootic growth of conotrolled Galton–Watson processes.

Annals of Probability, 13(4):1157–1178.

Mendolia, S., Stavrunova, O., and Yerokhin, O. (2021). Determinants of the community mobility during the COVID-19 epidemic: The role of government regulations and information. *Journal of Economic Behavior and Organization*, 184:199–231.

Milani, F. (2021). COVID-19 outbreak, social response, and early economic effects: A global VAR analysis of cross-country interdependencies. *Journal of Population Economics*, 34:223–252.

Qiu, Y., Chen, X., and Shi, W. (2020). Impacts of social and economic factors on the transmission of coronavirus disease 2019 (COVID-19) in China. *Journal of Population Economics*, 33:1127–1172.

Rungcharoenkitkul, P. (2021). Macroeconomic effects of COVID-19: A mid-term review. *Pacific Economic Review*, 26:439–458.

Shao, W., Xie, J., and Zhu, Y. (2021). Mediation by human mobility of the association between temperature and covid-19 transmission rate. *Environmental Research*, 194:110608.

Watanabe, T. and Yabu, T. (2021). Japan's voluntary lockdown: further evidence based on age-specific mobile location data. *Japanese Economic Review*, 72:333–370.

Wilson, D. J. (2021). Weather, mobility, and COVID-19: A panel local projections estimator for understanding and forecasting infectious disease spread. *Federal Reserve Bank of San Francisco Paper*, 2020-23.

Xiong, C., Hu, S., Yang, M., Luo, W., and Zhang, L. (2020). Mobile device data reveal the dynamics in a positive relationship between human mobility and COVID-19 infections. *Proceedings of the National Academy of Sciences*, 117(44):27087–27089.